INFINITE PERIOD BIFURCATION DUE TO IMPERFECTIONS IN ROTATING THERMAL CONVECTION

Jose Manuel Løpez Alonso

Tutor: Francisco Marques Truyol

Departament de Física Aplicada, Universitat Politècnica de Catalunya. 08034 Barcelona, Spain.

Abstract

A pinning area is a band of finite width where rotating waves with precession frequences near zero turn into steady non-axisymmetric solutions. Dynamical systems theory suggests that any imperfection breaking the $SO(2)$ invariance of a problem must result in the formation of such a region. Numerical simulations of rotating convection in a finite cylinder have been made breaking the symmetry by imposing a linear profile of temperature at the top lid in order to find the aforementioned steady solutions region.

Keywords: bifurcations, imperfections, rotating convection, dynamical systems theory

1 Introduction

Since the beginning of the 1980's decade dynamical systems theory has been used to understand the behavior of systems as parameters are varied which has allowed us to detect many bifurcations previously observed in experiments.
One of the most relevant elements in dynamical systems theory are symmetries. They reduce the complexity of the problem and determine the nature and type of bifurcations that a system can undergo. That is why many studies about bifurcations with symmetry have been carried out providing a deep comprehension of their dynamics. However, these analysis represent a group of idealized problems and don't take into account elements such as imperfections or noise that appear in real cases. Theoretical, experimental and numerical works have been performed recently in order to understand the dynamic caused by imperfect symmetries shedding new ligth on the problem.
An interesting particular case of symmetry is the invariance under rotation around an axis(SO(2) equivariant dynamical systems). In these systems Hopf bifurcations result in rotating waves with a precession frequency which depends on parameters. As we moved these parameters the precession frequency can pass through zero changing the sense of rotation in the wave. This situation is very sensitive to imperfections that break the SO(2) symmetry, giving rise to a band of finite width about the zero frequency line of the perfect system where the rotating waves become trapped turning into steady solutions. This is the so-called *pinning phenomenon*.
Pinning areas have been observed in physical experiments(Abshagen *et al.*, 2008) where imperfections appear in a natural way , however, numerical simulations of the symmetric systems were unable of detecting this kind of bifurcation. Later, Pacheco(Pacheco *et al.*, 2011) considered to break the symmetry of a Taylor Couette flow by tilting one of the endwall by a small angle. Numerical simulations of Navier Stokes equations for this modified system showed a band of steady solutions confined between two infinite period bifurcation curves. These results achieved a good agreement with the experimental ones, becoming evident that the pinning phenomenon is inherent to imperfections. With regards to theorical works, a detailed analysis of a system close to a Hopf bifurcation whose frequency changes sign has been performed by Marques(Marques *et al.*, 2011). It presents several ways of breaking the symmetry by introducing new terms up to second order into the normal form of the bifurcation. In all cases a pinning band delimited by infinite period bifurcation curves of homoclinic type appears around the zero frequency line.

On the other hand, the dynamic of a rotating cylinder subjected to a thermal gradient has been widely studied by the group of fluids at the UPC(Marques *et al.*, 2007);(Marques & Lopez, 2009). The linear stability analysis determined the existence of a rotating wave whose precession frequency undergoes a change of sign. This point suggests the presence of a pinning region in case that imperfections are present.

Taking advantage of the previous jobs, we considered to break the symmetry of the aforementioned cylinder by imposing a linear profile of tempeture at

the top lid in order to simulate the imperfections. After numerous numerical simulations of the flow inside the cylinder, we found the pinning area and established the infinite period bifurcation curves that surround it. These curves as well as the steady solutions arising as a consequence of the bifurcation will be shown in the section corresponding to results. An analysis to try to identify the type of global bifurcation which is happening is also exposed.

2 Governing equations and numerical scheme

Consider a cylinder of radius r_0 and height h rotating around a vertical axis with a constant angular velocity ω rad s^{-1} and filled with an incompressible fluid of kinematic viscosity ν. The top lid is manteined at a constant temperature $T_0 - 0.5\Delta T$ and the bottom lid at a constant temperature $T_0 + 0.5\Delta T$, being T_0 the mean temperature in the cylinder and ΔT the difference of temperature between the lids.
This problem depends on five non-dimensional independent parameters:

Rayleigh number

$$R = \frac{\alpha g h^3 \Delta T}{\kappa \nu} \tag{1}$$

Coriolis number

$$\Omega = \frac{\omega h^2}{\nu} \tag{2}$$

Froude number

$$F = \frac{\omega^2 r_0}{g} \tag{3}$$

Prandtl number

$$\sigma = \frac{\nu}{\kappa} \tag{4}$$

Aspect ratio

$$\gamma = \frac{r_0}{h} \tag{5}$$

where α is the coefficient of volume expansion, g is the gravitational acceleration and κ is the thermal diffusivity.
A whole analysis of the problem including these five parameters would be impossible so we have fixed some parameters. We have chosen $\gamma = 1$ because large azimuthal wavenumber modes are avoided, $\sigma = 7.0$ which corresponds to water near room temperature and $\Omega = 100.0$. Notice that since Ω and F depend on ω, they vary at the same time, however, we will consider a fixed Coriolis number in order to reduce the complexity of the problem. In that way, we are considering to study the competition arising between gravitational buoyancy(characterized by R) and centrifugal buoyancy(characterized by F).
The governing equations of the problem have been non-dimensionalized using h as a length scale, $\frac{h^2}{\kappa}$ as the time scale and ΔT as the temperature scale. In a rotating frame of reference, they are:

$$\nabla \cdot \mathbf{u} = 0, \tag{6}$$

$$(\partial_t + \mathbf{u}\cdot\nabla)\mathbf{u} = -\nabla p + \sigma\nabla^2\mathbf{u} + \sigma R\Theta\hat{z} + 2\sigma\Omega\mathbf{u}\times\hat{z} - \frac{\sigma F R}{\gamma}\Theta\mathbf{r}, \tag{7}$$

$$(\partial_t + \mathbf{u}\cdot\nabla)\Theta = w + \nabla^2\Theta \tag{8}$$

where $\mathbf{u} = (u, v, w)$ is the velocity field in cylindrical components (r, θ, z), p is the kinematic pressure(including centrifugal and gravitational contributions), $\hat{z}$ is the unit vector in the vertical direction z and $\mathbf{r}$ is the radial vector in cylindrical components. In the equation 8 a non-dimensional temperature has been substituted by the unknown Θ that represents the deviation of the temperature respect to the conductive state. This practice is usual in thermal convection studies. The Boussinesq aproximation has been taken into account in such formulation so that all fluid properties are constant except for the density which depends on the temperature in the gravitational and centrifugal terms.
The boundary conditions for $\mathbf{u}$ and Θ are:

$$r = \gamma : \Theta_r = u = v = w = 0, \tag{9}$$

$$z = \pm 1/2 : \Theta = u = v = w = 0, \tag{10}$$

This set of equations with its boundary conditions is invariant under rotations around the axis of the cylinder. It doesn't take into account the imperfections which lead the systems to bifurcate in a pinning region. In order to introduce these imperfections in the system, a linear profile of temperature has been placed at the top lid. The new boundary condition break the invariance mentioned before simulating the effect of imperfections in real experiments.It can be expressed as:

$$z = +1/2 : \Theta = \epsilon r cos\theta, \tag{11}$$

where ϵ is an arbitrary constant.
The code used to solve the problem have been implemented by the convective and rotational instabilities

group at the UPC(Mercader *et al.*, 2010). It consists in a second-order time-splitting method for the time discretization combined with a pseudo-spectral method using Galerkin-Fourier in the azimuthal component θ and Chebyshev collocation in $x = r/\gamma$ and $y = 2z$ for the spacial discretization. Each unknown of the problem can be written as follows:

$$F(r,\theta,z) = \sum_{l=0}^{L}\sum_{n=0}^{N}\sum_{m=0}^{M} a_{l,n,m} T_l(x) T_n(y) e^{im\theta} \quad (12)$$

The radial dependence is approximated by a Chebyshev expansion between $-\gamma$ and γ and enforcing their proper parities at the origin. An odd number of Gauss-Lobatto points have been chosen in r to avoid including the origin in the collocation mesh, therefore the equations are solved only in the interval $(0, \gamma]$. Linear diffusion terms in momentum equations have been decoupled by using the combinations $u_+ = u + iv$ and $u_- = u - iv$. For each Fourier mode, a set of Helmholtz equations arises for T,w,u_+ and u_-. They are solved by mean of a diagonalization technique in r and z. Finally, steady solutions are computed by Newton's method and steady solutions branches are followed by an arclength continuation method.

A slight modification have been introduced in the code to consider the new boundary condition at the top lid. In order to do that, the physical condition had to be turned into a spectral condition. Particularly, introducing a linear profile of temperature means to modify the azimuthal mode $m = 1$.
We have used $L = N = 36$ spectral modes, $M = 20$ in θ and $\delta t = 10^{-5}$ in all simulations. The proper spectral convergence of the code with this number of modes have been checked in previous works.

3 Results

Before explaining the results achieved in this work, it is necessary to introduce background information relative to the linear stability analysis of the problem. The bifurcations of the stable state $C0$ (called centrifugal branch) are shown in figure 1. This solution becomes unstable at a Hopf bifurcation(H^3_{CO}) to a rotating wave with azimuthal wavenumber $m = 3$(C3). At low R numbers this Hopf bifurcation is supercritical but when they become larger, a Bautin point(B) appears turning the supercritical Hopf bifurcation into a subcritical one. Unstable solutions($C3$) appear due to the subcritical nature of the bifurcation, becoming them stable at a saddle node(F^u_{C3}) born as well at the Bautin point.

Figure 2 shows how the Hopf frequency corresponding to H^3_{C0} varies as we move R. This Hopf frequency(ω) comes given by the imaginary part of

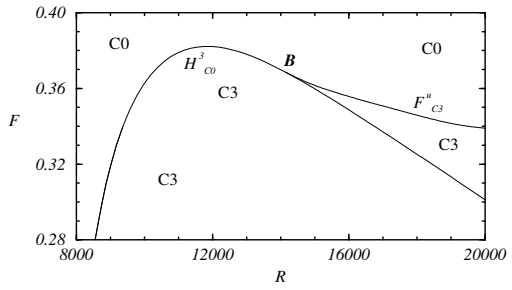

Figure 1: Bifurcations of the centrifugal branch $C0$.

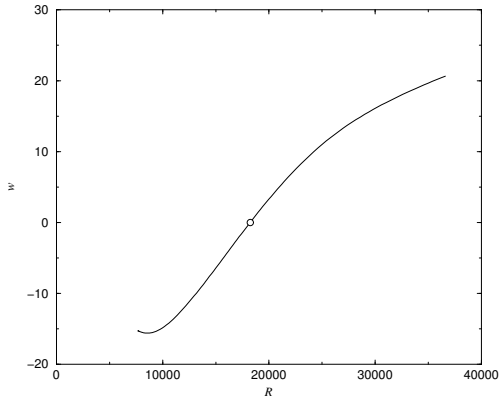

Figure 2: Hopf frequency against Rayleigh number.

the critical eigenvalue and it is closely related to the precession frequency ω_p of the rotating wave. Namely, it can be expressed as $\omega_p = \omega/3$. If we look at the figure, there exist a value of R where ω passes through zero what implies a change in the rotation sense of the rotating wave. This is the point $(R, \omega) = (18234, 0)$ represented in figure 2 as a white circle. The existence of this point means the starting point of this work. It suggests that in presence of imperfections, rotating waves with very low ω_p may be stopped by them, giving rise to steady solutions. Moreover, the dynamical system theory says that period infinite bifurcations delimit the area where this happens.
The first step in order to find this region is to look for several points with $\omega_p = 0$ in the perfect problem(without breaking the symmetry). We could think of finding them in the neighborhood of the previous point($R \simeq 18234$) but if we look at the figure 1, that interval of R belongs to the subcritical part of the bifurcation so rotating waves close to this point will be unstable. Our code is only able of computing stable solutions so we had to explore the phase space up to find stable rotating waves with zero precession frequency.
To calculate ω_p, we have used a small code that considers two close solutions , evaluates the phase difference between them and finally divides by δt

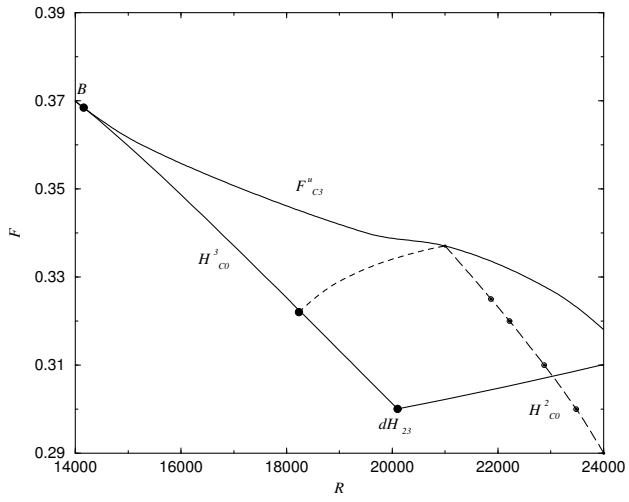

Figure 3: Line of rotating waves with ω_p=0.

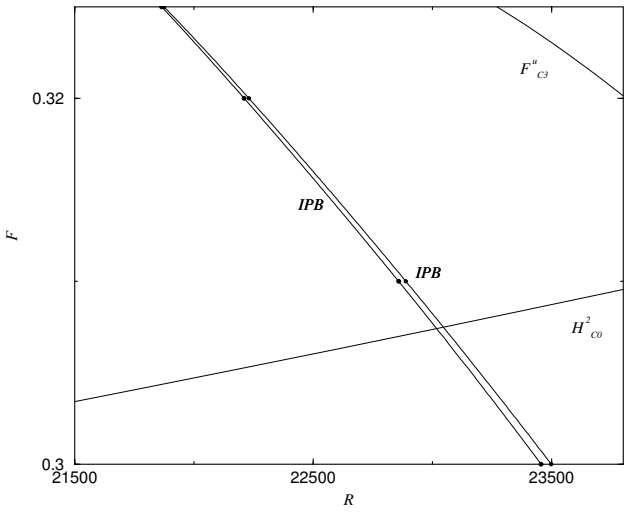

Figure 4: Pinning area.

and the azimuthal wavenumber corresponding to the rotating wave(In this case 3).

Figure 3 shows the results obtained in the exploration. The dashed line represents solutions with zero precession frequency. Rotating waves change their sense of rotation when they are passing through it. As we said before, we only have calculated stable solutions which are represented to the right of the graph by a long dashed line. The points obtained in the simulations are also shown. Unstable solutions are also represented in the figure by the short dashed line but they have been drawn by hand in order to clarify what is happening in the system.
Once we know the region of the phase space where ω_p is close to zero, it is time to introduce the new boundary condition to break the $SO(2)$ invariance of the problem. A new exploration close to the previous line was carried out. The results are shown in figure 4. The small band between the two IPB curves is the pinning area. In this region rotating waves become a non-axisymmetric steady state.

What kind of bifurcation is happening?

Dynamical system theory predicts an infinite period bifurcation(IPB).In order to prove it, we have calculated several points with constant $F = 0.32$ and varying R very close to the IPB curve. Figure 5 presents the periods corresponding to those points against R. As we moved R closer to the pinning area the periods tend to infinite, that is why this kind of bifurcations are called infinite period bifurcation. A detailed theoretical study of this bifurcation can be found in (Marques *et al.*, 2011). It shows that two solutions arise when a limit cycle enters the pinning region and they are born at saddle-node bifurcations. One is a saddle and the other is stable. The stable solution is the only one that can be observed numerically when using time evolution, in fact, we will show it later in this report. The unstable one corresponds to a saddle-node which is connected to the stable periodic solutions located on both sides of the pinning region via saddle node on an invariant cycle($SNIC$) bifurcations.
An example of the path followed by the basic state $C0$ as we moved F and R is large enough is shown in figure 6. From A to A', $C0$(region I) undergoes first a Hopf bifurcation to a rotating wave $C3$ with counterclockwise sense of rotation(region I_+), next , it goes to a pinning area where we have the pinned steady solutions(region III) and finally, it bifurcates to a rotating wave $C3$ again but with opposite sense of rotation to the previous one(region I_-). The gray disks placed between the $SNIC$ and Hopf curves are areas of extremely complex dynamic. Many other bifurcations appear in this narrow region of the parameter space making very difficult to try to investigate it.

This is the most likely scenario that can be found in real systems, however, when the $SNIC$ bifurcation curve is close to the Hopf bifurcation(gray disks in figure 6), saddle node bifurcations are no longer happen on the limit cycle. A homoclinic collision between the limit cycle and the saddle node occurs in such situation but saddle node bifurcations are still very close to it. Since they are very close to each other is very difficult to distinguish between them. One way to do that is checking the scaling laws of the periods when approaching a homoclinic or a $SNIC$ bifurcation. They come given by the following expressions(Strogatz, 1994):

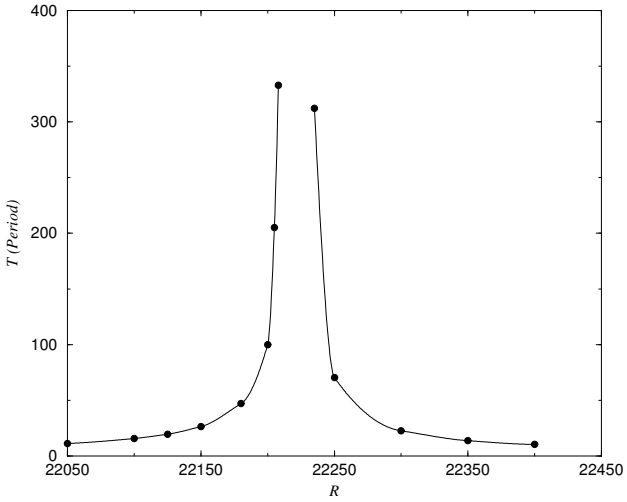

Figure 5: Period T vs R close to the pinning area. $F = 0.32$.

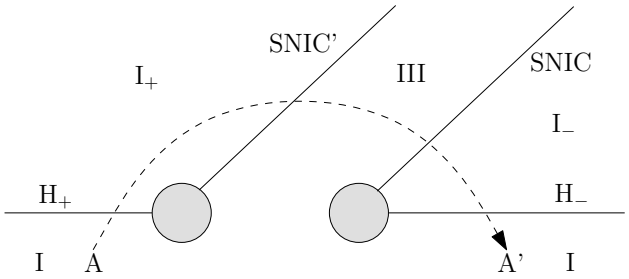

Figure 6: Imperfect Hopf bifurcation under general perturbations.

$$T_{HOM} = a_1 - a_2 \ln(a_3 - x) \tag{13}$$

$$T_{SNIC} = a_1 + \frac{a_2}{\sqrt{a_3 - x}} \tag{14}$$

where x means the control parameter(in our case R). The parameter a_2 of the homoclinic scaling law has a physical meaning. It represents the inverse of the positive eigenvalue of the saddle-node.

By following these guidelines, we have tried to identify the situation happening in our case. A non-linear fitting of the periods corresponding to points near the IPB curve have been performed obtaining the result shown in figure 7. As we can see the square root profile fits slightly in a better way than the logarithmic one. This cannot be interpreted as a reliable proof to ensure that a $SNIC$ bifurcation is happening because we would need periods corresponding to points located in a very narrow region of parameter space whose width is of the order of the distance between both curves(saddle node and homoclinic). These points are difficult to compute accurately and because of their large periods, it takes a long time to do it. Anyway, it is highly probable that a $SNIC$ bifurcation exists in our case.

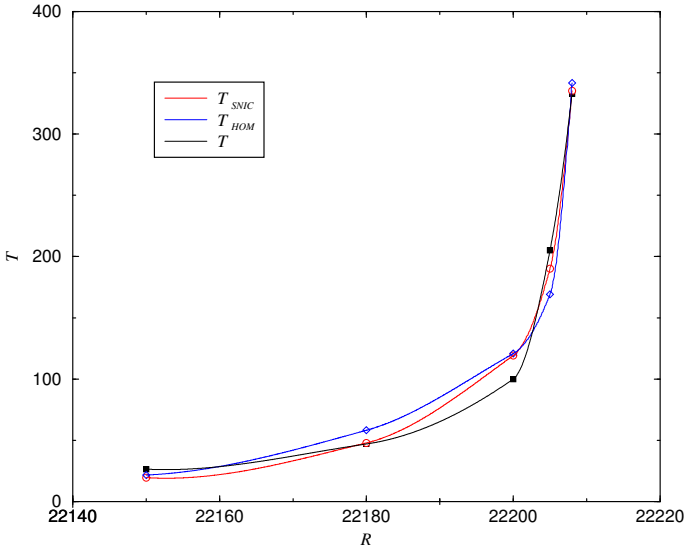

Figure 7: Non-linear fitting of periods corresponding to points near the pinning area. In color version, red line represents the $SNIC$ scaling law(points represented as circles) and blue line is the logarithmic adjust(points marked by diamond). Black line represents the original points numerically calculated.

Time series of the temperature were also measured at a point close to the wall and over the half plane of the cylinder. Two first pictures in figure 9 shows time series corresponding to points inside the pinning region. We can appreciate how the temperature is going to a steady solution in both cases after an initial relaxation time. It is noticiable that this relaxation time becomes larger as F is increased. Last two pictures compare the period in a point very close to the pinning area(third picture, $R = 22205$ and $F = 0.32$) and another one a little further (fourth picture, $R = 22180$ and $F = 0.32$).

Finally, we present some characteristics of the steady solution obtained. Figure 8 shows isotherms T plotted in meridian planes, with $R = 22875$ and Froude number $F = 0.31$, for different angles. The rotating wave resulting from the Hopf bifurcation is composed of three hot rising and three cold descending plumes near the sidewall and preccesing retrograde with respect to the system rotation. Its effects can be straightforward appreciated in the figure, as we moved θ we see how the temperature near the wall is changing. Picture (a) and picture (c) show clearly the effects of the hot and cold plumes respectively. Notice that cool fluid at the top of the cylinder is centrifuged radially outward while warm fluid near the bottom is centrifuged radially inward. The hot and cold plumes arising make the effects of centrifugal forces smoother on the sidewall. This solution is rotating for most

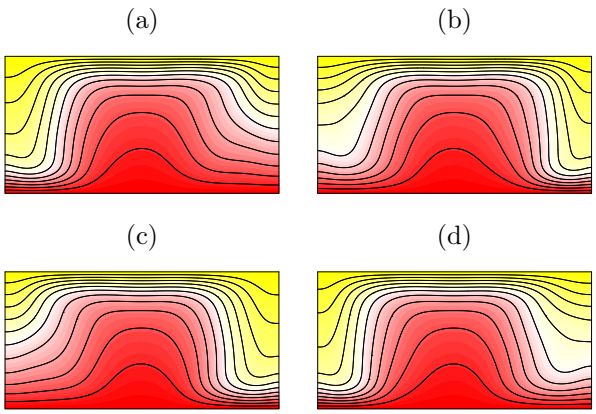

Figure 8: Isotherms of the state $C3$ at $R = 22875$ and $F = 0.31$, in a meridional plane where the left and right vertical boundaries shown are the cylinder sidewall at $r = \gamma$ and θ is changing: (a) $\theta \in [0, 180]$, (b) $\theta \in [30, 210]$, (c) $\theta \in [60, 240]$ (d) $\theta \in [90, 270]$. There are ten contour levels linearly spaced, five positives(black or red in colour version) and five negatives(gray or yellow in colour version) in the range $T \in [-0.5, 0.5]$

part of the parameter space where it exists, but as we saw before it becomes steady in the small band presented in 4.

4 Conclusions and future works

Numerical simulations of a fluid enclosed in a rotating cylinder in the presence of a thermal gradient have been carried out. Imperfections breaking the $SO(2)$ invariance of the problem have been considered by introducing a linear profile of temperature at the top lid of the cylinder as a new boundary condition. The most important feature achieved is that the curve of zero frequency relative to the periodic stable solution($C3$) splits into two curves with a region of zero-frequency solutions appearing in between(the so-called pinning area). These outcomes confirm the theoretical results obtained previously which ensure the presence of a steady solutions band when imperfections are considered in a problem where the precession frequency of a rotating wave is changing sign.

A couple of interesting works to do in the future related to this job are:

- Try to calculate the unstable solutions mentioned in section three.
- Break the SO(2) invariance in other way to see if the band becomes wider.

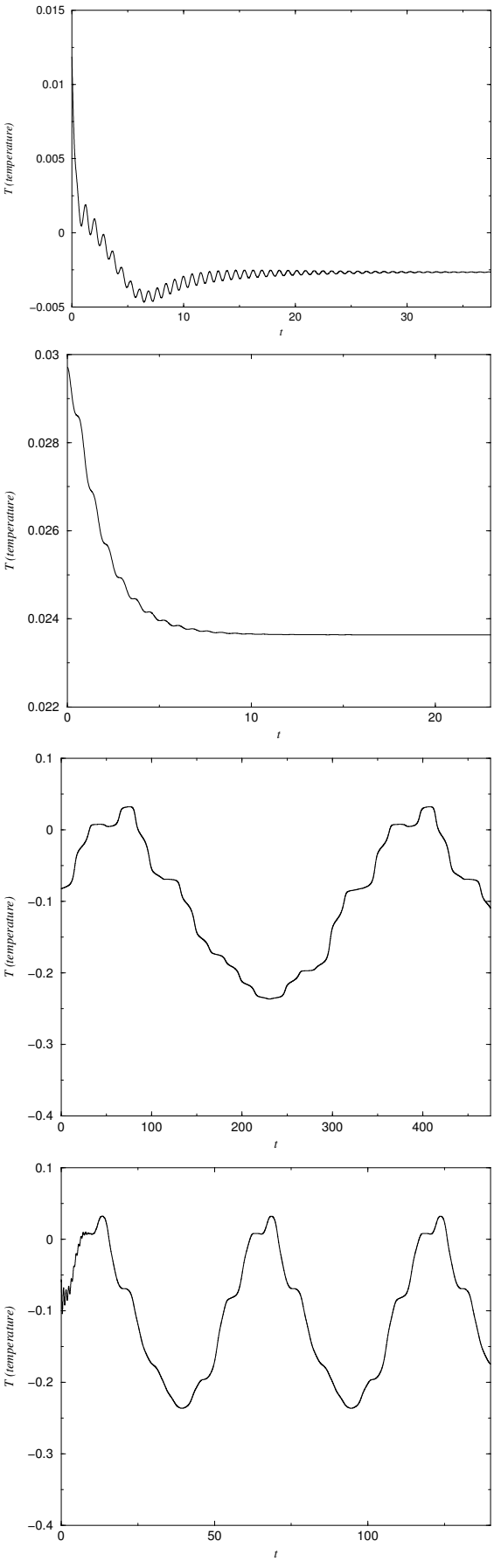

Figure 9: From top to bottom, $(R, F) = (21874, 0.325)$, $(R, F) = (22868, 0.31)$, $(R, F) = (22205, 0.32)$ and $(R, F) = (22180, 0.32)$.

References

Abshagen, J., Heise, M., Hoffmann, C. & Pfister, G. 2008 Direction reversal of a rotating wave in taylor-couette flow. *Journal of Fluid Mechanics* **607**, 199– 208.

Marques, F. & Lopez, J. M. 2009 Centrifugal effects in rotating convection: nonlinear dynamics. *Journal of Fluid Mechanics* **628**, 269–297.

Marques, F., Mercader, I., Batiste, O. & Lopez, J. M. 2007 Centrifugal effects in rotating convection: axisymmetric states and three-dimensional instabilities. *Journal of Fluid Mechanics* **580**, 303–318.

Marques, F., Meseguer, A., Lopez, J. M. & Pacheco, J. R. 2011 Hopf bifurcation with zero frequency and imperfect so(2) symmetry. *Submitted to Elsevier* .

Mercader, I., Batiste, O. & Alonso, A. 2010 An efficient spectral code for incompressible flows in cylindrical geometries. *Computers & Fluids* **39**, 215–224.

Pacheco, J. R., Lopez, J. M., & Marques, F. 2011 Pinning of rotating waves to defects in finite taylor-couette flow. *Journal of Fluid Mechanics* **666**, 254–272.

Strogatz 1994 *Nonlinear Dynamics and Chaos*. Perseus Books.